J. Chem. Tech. Biotechnol. 1979, **29**, 1–7

Magnetic and Catalytic Properties of Sintered Nickel Catalysts for the Methanation Reaction

Raymond C. Everson[a], Laxman N. Mulay,
Om P. Mahajan and Philip L. Walker, Jr

Material Sciences Department, The Pennsylvania State University, University Park, Pa 16802

(Paper received 19 June 1978 and accepted 15 September 1978)

Ni catalysts supported on Al_2O_3, as received commercially and subjected to sintering at 723–973 K, were characterised in terms of distinct magnetic structures. It was found that the Ni on all the catalysts consisted of a mixture of single domain structures, with and without anisotropic effects, and multidomain (ferromagnetic) structures. The formation of the multidomain particles during the sintering process coincides with a decrease in catalytic activity for the reaction $CO + 3H_2 \rightarrow CH_4 + H_2O$. From this study it was concluded that the methanation reaction is 'magnetic-structure' sensitive.

1. Introduction

Supported catalysts prepared by different methods with large amounts of metal normally have complicated metal dispersions, consisting of regular and irregular isolated particles of different sizes together with porous clusters and 'islands' of varying dimensions.[1] When catalysts of this nature are subjected to sintering temperatures, a complicated mechanism of crystal growth occurs, which results in a rather ill-defined metal dispersion. Under these conditions, characterisation by a particle size distribution would be inadequate; an exact determination would be impossible. However, in the case of 3d transition metals, as used for industrial methanation and Fischer–Tropsch synthesis, it is possible to characterise dispersions by the estimation of the relative amounts of certain magnetic structures, which have distinct physical and electronic properties. The three types of magnetic structures which normally coexist on supported Fe, Ni and Co catalysts at temperature below the respective Curie temperatures are as follows.

The so-called 'superparamagnetic' particles[2] consist of single magnetic domains, characteristic of very small particles, and have magnetisation curves described adequately by the Langevin equation. The magnetisation is strongly particle-size dependent and can actually be used for the assessment of the average metal particle size.

Single domain particles can have anisotropic contributions to their energy arising from their external shape and crystalline structure, thus constituting a distinct structure characterised by a significant hysteresis; these are labelled single domain–anisotropic in this paper.

The third kind of structure, characteristic of bulk 3d metals, consists of multidomain particles displaying a distinct change at the Curie temperature to a paramagnetic structure.

The effect of any change in the internal magnetic characteristics on the catalytic activity, known as the 'Hedvall effect' has been well established for some reactions.[3] The effect can occur in either of two detectable manners. Hedvall I appears as a discontinuity in an Arrhenius plot and Hedvall II as a change in the slope of this plot. Both occur at the change-over from one structure to another, such as multidomain structures to paramagnetic structures at the Curie point. The question now is whether the magnetic structures mentioned above have different specific catalytic activities

[a] Present address: Department of Chemical Engineering, University of Natal, Durban, South Africa.

0142-0356/79/0100-0001 $02.00

over the same temperature range or whether the methanation reaction over nickel is 'magnetic structure' sensitive or not.

Investigations of the problem of dependance of specific catalytic activity on structure were first carried out by Boreshov *et al.*[4] and later extended extensively.[5–7] These investigators reported reactions which showed distinct sensitivity to structure for some well-dispersed catalyst systems of platinum and iron.

In this paper some typical results on two commercial-grade Ni/Al_2O_3 catalysts are presented with special reference to (a) the change in magnetic structure composition upon sintering at elevated temperatures and (b) correlation of such changes with corresponding energies of activation, E.

2. Experimental

2.1. Apparatus for chemical activity

A packed bed, continuous flow, microreactor was used to obtain data. It was made of silica glass tubing (1.2 cm i.d.) with a concentric air jacket (with an annulus of about 0.5 cm gap) required for temperature control of the reaction. An electric furnace surrounded the air jacket, the packing and a preheating section ahead of the reaction zone. By using different air flow-rates from a compressed air supply, it was possible to stabilise reaction temperatures for a very wide range of operating conditions. Catalysts in the form of a fine powder were supported on a stainless steel gauze held firmly inside the reactor tube.

The product stream was analysed using a Hewlett Packard chromatograph with thermal conductivity detection together with a column of 100–120 mesh fraction of Carbo Sieve B. The column was operated at 325 K with a hydrogen–helium carrier gas at 40 $cm^3\ min^{-1}$. This reactor could be operated at temperatures up to 1000 K at atmospheric pressure and was used for reduction, reaction and sintering. Reactions were carried out at 548–673 K.

2.2. Apparatus for magnetic measurements

A vibrating sample magnetometer, supplied by Princeton Applied Research Corporation, was used for all the measurements. Magnetic fields up to 20 kG were generated and measured with a separate gaussmeter inserted between the magnetic poles and very close to the vibrating sample. For high temperature measurements a platinum-wound furnace surrounded by a water jacket, to prevent damage to the detection coils, was used. Low temperature measurements were accomplished with liquid nitrogen and solid carbon dioxide contained in a Dewar flask and surrounding a sealed glass tube in which the samples vibrated.

2.3. Catalyst samples

Two commercially available Ni/Al_2O_3 catalysts 'A' and 'B', prepared by different methods, with physical characteristics listed in Table 1, were available for this investigation. Sintered specimens for the magnetic measurements were obtained from the packed reactor described above with a synthesis gas containing 17 mol% carbon monoxide in hydrogen. The conditions under which sintering occurred consisted, firstly, of a reduction period of 1 h with flowing hydrogen at about 400 $cm^3\ min^{-1}$ at selected sintering temperatures, and secondly, of a reaction period also of 1 h duration at the selected sintering temperature.

Samples of the 'as received' and sintered pellets weighing between 40 and 50 mg were reduced again and sealed under vacuum in glass tubes before measurement on the magnetometer. The degree of metal dispersion was estimated with a conventional constant-volume hydrogen adsorption system.

3. Analytical methods

3.1. Quantitative magnetic analysis

The relative amounts of the three structures, namely, superparamagnetic, single domain–anisotropic and multidomain depend upon the observation temperature, which should be below the Curie

Table 1. Characteristics of catalysts as received and sintered

	Catalyst 'A'—43% Ni on γ-Al_2O_3				Catalyst 'B'—67% Ni on γ-Al_2O_3			
Sintering temperature (K)	As received	773	873	973	As received	773	873	973
BET area $m^2 g^{-1}$	51	—	—	—	117	—	—	—
Average crystallite size (nm) (111)	18.50	19.10	23.30	25.60	7.40	11.10	13.50	16.00
Superparamagnetic fraction	0.36	0.27	0.21	0.12	0.58	0.48	0.40	0.26
Mass of superparamagnetic particles g per g catalyst	0.155	0.116	0.090	0.051	0.394	0.326	0.272	0.177
Mean particle diameter of superparamagnetic fraction (nm)	2.50	2.90	5.40	3.70	2.40	2.50	2.80	2.60
Degree of metal dispersion % of total Ni atoms on surface	5.12	5.54	3.36	3.78	10.01	9.78	7.82	7.62

temperature (629 K). Active nickel catalysts at low reaction temperatures usually have negligible anisotropic contributions to the overall energy, thus a reference temperature within this range would be both convenient and informative. This choice incidentally eliminates the complex analysis required for single domain–anisotropic structures. Therefore, a system consisting of single domain particles all displaying superparamagnetism and multidomain particles with negligible hysteresis needs to be analysed.

The magnetisation curves for such systems show a steep slope in the low field region, like those of multidomain particles, whereas at high fields they approach saturation very slowly resembling the magnetisation curves of superparamagnetic particles. Thus, at high fields the total magnetisation is composed of a constant saturated component due to the multidomain fraction and a sloping component obeying the Langevin equation which is strongly particle-size dependant. Thus the equation for the high field magnetisation is given by[1]

$$\frac{\sigma}{\sigma_s} = \left(1 - \sum_i x_i\right) + \sum_i x_i L\left(\frac{I_{sp} v_i H}{T}\right) \tag{1}$$

The expressions under the summation signs refer to the superparamagnetic particles, L denotes the Langevin function and v_i the mean volumes of the particles within the x_i fraction. This equation can be fitted conveniently, by a regression routine, to experimental data with the evaluation of the fraction of superparamagnetic particles Σx_i and a mean particle volume $\bar{v}$ as proposed by Selwood.[8] The Langevin for this case would thus simply be

$$L\left(\frac{I_{sp}\bar{v}H}{T}\right) \tag{2}$$

3.2. Analysis of the rate of methanation

The following procedure was adopted for the examination of 'magnetic structure' sensitivity, under steady-state operation without deactivation, and under conditions such that significant conversions were obtained: (a) determination of a suitable rate equation, and (b) construction of an Arrhenius plot.

The literature[9] has many forms of the rate equation for methanation, expressed either in terms of carbon monoxide consumed or methane formed, over temperature and pressure ranges of 493–973 K and 1–70 bar, respectively.

The following two rate equations developed by Lee[9, 10] appeared most suitable for this investigation: (a) the rate of consumption of carbon monoxide, given by

$$r_{CO} = k_1 \exp(E/RT) p_{CO}^{0.62} \tag{3}$$

and (b) the rate of methane formation, incorporating the effects of methane and hydrogen present in the reaction mixture, given by

$$r_{CH_4} = \frac{k_2 \exp(E/RT) p_{CO} p_{H_2}^{0.5}}{1 + 0.1\, p_{H_2} + 0.05\, p_{CH_4}} \tag{4}$$

The coefficients 0.1 and 0.05 in the denominator of this equation were evaluated[10] from data obtained from a large number of catalysts tested in a CSTR within a very wide range of variables.

4. Results and discussion

4.1. Magnetic analysis of dispersions at an elevated temperature

A reference measuring temperature of 573 K was chosen for the following reasons. Firstly, it is below the Curie point (629 K) at which significant magnetisation can be observed and secondly, most samples displayed characteristics that could be analysed by the method previously proposed[11] and outlined above. Below this temperature significant hysteresis occurs indicating distorted metal particles thus constituting a single-domain–anisotropy structure, as indicated in Figure 1.

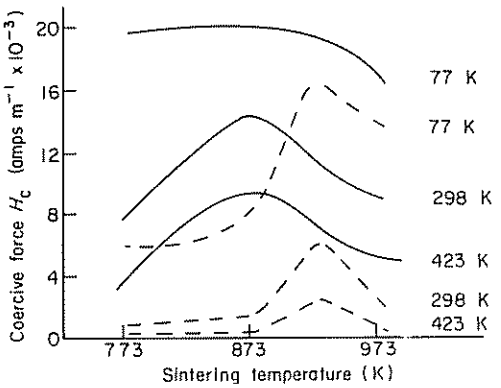

Figure 1. Coercive force as a function of sintering temperature. ——, Catalyst 'A'; – – –, catalyst 'B'. (The temperatures of measurement for the catalyst are shown next to the curves.)

A non-linear regression computer programme incorporating a hill-climbing procedure for the estimation of the parameters Σx_i and $\bar{v}$, as given by equations (1) and (2), converged very rapidly to unique values.

Estimates of the fractions of superparamagnetic particles, relative to the total metal present in the catalysts, and mean particle diameters within the superparamagnetic fractions only and the degree of metal dispersion are shown in Table 1. For the calculation of mean particle diameters it was assumed that the particles are spherical. The increased transformation to multidomain particles (bulk) at high temperatures is evident. The loss of surface atoms as a result of growth is thus accompanied by marked magnetic structural changes. The changes in the mean particle sizes are not so marked and are smallest for catalyst 'B', which contains the most metal. Previous results obtained[1] were at much lower temperatures, i.e. 90 and 290 K, and used an approximate distribution for the particle sizes consisting of a number of discrete constrained values. These workers[11] also used magnetic properties for an investigation showing marked differences in supported Ni prepared from different salts, i.e. formates, oxalates and carbonates.

The actual mass of superparamagnetic particles per unit mass of catalyst is given in Table 1. It can be seen that the most sintered sample of catalyst 'B' had more fine particles than catalyst 'A'. Also, because of the larger metal loading on catalyst 'B', a larger overall weight of Ni was converted at any sintering temperature.

Mean crystallite sizes of the Ni, as determined by X-ray diffraction are also given in Table 1.

4.2. Catalytic activity

A large number of experiments were conducted on powdered catalysts of about 0.350 g within the range 100–170 mesh. This size was established by examination of the activities of catalysts of difference sizes. The size range over which no change in activity was detected indicated no intraparticle diffusion limitations. The flow rate of the synthesis gas was varied from 400 to 1800 $cm^3\ min^{-1}$, similar to that used in other work[12] and much greater than that used by Vannice.[13] It was assumed that under these conditions the effect of diffusion to and from the particle surfaces was negligible.

Table 2 shows some yields of methane obtained at atmospheric pressure with a synthesis gas containing 17% carbon monoxide in hydrogen ($CO:H_2 = 1:4.7$). The performances of the 'as received' catalyst and the most sintered catalyst (i.e. at 975 K) were compared. A remarkable decrease was detected at 548 and 573 K for catalyst 'A', to a practically inactive catalyst, whereas the change was only marginal for catalyst 'B'.

Table 2. Methane yields as % (by volume) in dry product stream on 0.350 g catalysts and flow-rate of 837 $cm^3\ min^{-1}$

	Catalyst 'A'		Catalyst 'B'	
Temperature (K)	As received	Sintered at 973 K	As received	Sintered at 973 K
673	14.3	10.5	25.3	25.3
648	13.6	9.2	24.7	24.5
623	12.8	7.2	24.0	23.7
598	11.3	5.0	24.0	22.5
573	9.7	≒0.0	22.4	20.9
548	7.5	0.0	21.0	19.7

For the synthesis gas used and the conversions obtained it was thermodynamically impossible for any carbon deposition.[14] This was confirmed by the fact that the same catalyst did not show any deactivation when experiments were repeated after long reaction periods under varying conditions. Also steady state operation was obtained almost instantaneously.

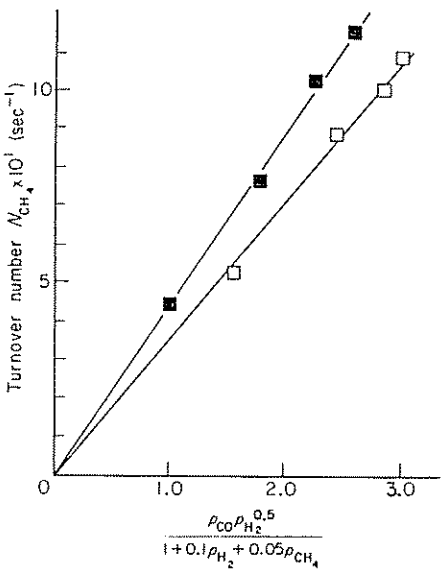

Figure 2. Rate of methane formation at 673 K for catalyst 'A': (■) as received; (□) sintered at 973 K. Pressures in psia in order to compare directly with previous work.[10]

Rate data in terms of turnover numbers were correlated with many published rate equations.[9, 10] It was found that no one particular equation fitted all the results obtained from the two catalysts 'A' and 'B'. Instead, the rate equations (3) and (4) described the behaviour of catalyst 'B' and 'A' ('as received' and sintered) respectively exceptionally well (Figures 2 and 3). These two plots are from data at 673 K and the difference between the 'as received' and sintered catalysts is clearly seen. The fact that different rate equations hold for different catalysts under exactly the same reaction conditions is indeed of great interest.

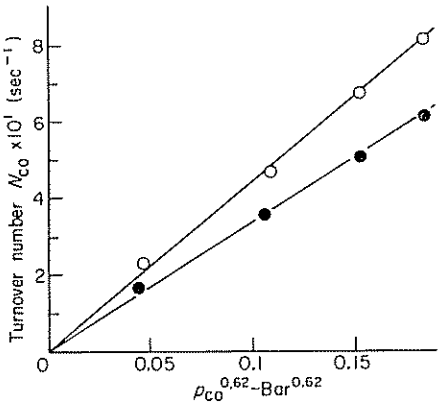

Figure 3. Rate of carbon monoxide conversion at 673 K for catalyst 'B': (●) as received; (○) sintered at 973 K.

Arrhenius plots for the two catalysts (Figures 4 and 5) clearly show the difference between the 'as received' and sintered samples. It is interesting to note that the activation energy reported by Lee[10] of 28.98 kJ mol^{-1} (E_{CH_4}) compares well with that determined for catalyst 'A' 'as received'. Vannice[15] reported results for (E_{CH_4}) obtained by other investigators which varied from 10.1 to 134.4 kJ mol^{-1}, but information concerning the exact physical properties of the catalysts is not available which would provide a meaningful comparison. The activation energies (E_{CO}) for catalyst 'B' are very low when compared with published results,[10, 13] this however could be characteristic of the method of catalyst preparation and the resultant Ni dispersion (67%) examined.

The change in the activation energy especially for catalyst 'A' supports the view that the activity of the multidomain particles despite its low active site population has a low activity.

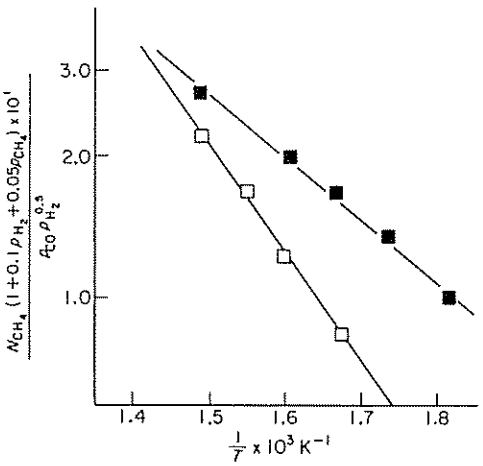

Figure 4. Arrhenius plot for catalyst 'A': (■) as received $E=25.746$ kJ mol^{-1}; (□) sintered at 973 K $E=43.554$ kJ mol^{-1}.

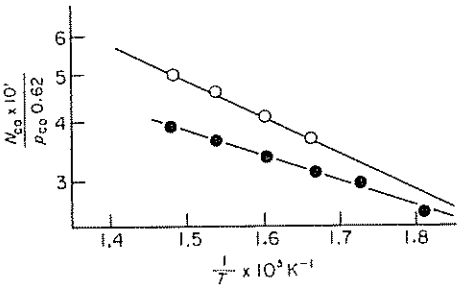

Figure 5. Arrhenius plot for catalyst 'B': (●) as received $E = 10.08$ kJ mol^{-1}; (○) sintered at 973 K $E = 14.406$ kJ mol^{-1}.

5. Conclusions

1. Industrial nickel catalysts can be characterised successfully in terms of magnetic structures.
2. Different rate equations hold for dispersions resulting from different methods of preparation.
3. An increase in the multidomain particle fraction on a nickel catalyst causes an increase in the energy of activation, indicating 'magnetic structure' sensitivity.

Nomenclature

E	Activation energy
H	Applied field
I_{sp}	Spontaneous magnetisation
k	Reaction rate constant
N	Turnover numbers, i.e. molecules formed or reacted per metal atom per second
p	Partial pressure
r	Rate of reaction
T	Temperature
v	Volume of superparamagnetic particle
$\bar{v}$	Mean volume of superparamagnetic fraction
x	Fraction of superparamagnetic particles
σ	Magnetisation
σ_s	Saturated magnetisation

References

1. Romanowski, W. *Z. Anorg. Allg. Chem.* 1967, **351**, 180.
2. Frenkel, J.; Dorfman, J. *Nature (London)*, 1930, **126**, 274.
3. Hedvall, J. A. In *Solid State Chemistry* Elsevier, Amsterdam, 1966, p. 78.
4. Boreskov, G. K.; Slinko, M. G.; Chesalova, V. S. *Zh. Fiz. Khim.* 1956, **30**, 2787.
5. Boudart, M.; Aldag, A.; Benson, J. E.; Dougharty, N. A.; Harkins, C. G. *J. Catal.* 1966, **6**, 92.
6. Brill, R.; Kurzidim, J. *Colloq. Int. CNRS* 1969, **187**, 99.
7. Ostermaier, J. J.; Katzer, J. R.; Manogue, W. H. *J. Catal.* 1974, **33**, 457.
8. Selwood, P. W. *Adsorption and Collective Paramagnetism* Academic Press, New York, 1962.
9. Lee, A. L.; Feldkirchner, H. L.; Tajbl, D. G. *Methanation for Coal Hydrogenation, Symposium on Hydrogen Processing of Solid and Liquid Fuels, Chicago* Am. Chem. Soc. Division of Fuel Chemistry (Joint with Division of Petroleum Chemistry, Inc.) September 1970, Preprints, 14, no. 4, Part I, p. 126.
10. Lee, A. L. *Symposium on Clean Fuel from Coal* IGT, 1973, 341.
11. Romanowski, W.; Dryer, H.; Nehring, D. *Z. Anorg. Allg. Chem.* 1961, **310**, 286.
12. Dalla Betta, R. A.; Piken, A. G.; Shelef, M. *J. Catal.* 1974, **35**, 54.
13. Vannice, M. A. *J. Catal.* 1975, **37**, 449.
14. Greyson, M.; Demeter, J. J.; Schlesinger, M. D.; Johnson, G. E.; Janakin, J.; Myers, J. W. *U.S. Bur. Mines, Rep. Invest.* 1955, no. 5137.
15. Vannice, M. A. *J. Catal.* 1975, **37**, 462.